Terahertz quantum cascade lasers with copper metal-metal waveguides operating up to 178 K

Mikhail A. Belkin[1*], Jonathan A. Fan[1], Sahand Hormoz[1], Federico Capasso[1*], Suraj P. Khanna[2], Mohamed Lachab[2], A. Giles Davies[2], and Edmund H. Linfield[2]

[1]*Harvard School of Engineering and Applied Sciences, Harvard University, Cambridge, MA 02138*
[2]*School of Electronic and Electrical Engineering, University of Leeds, Leeds LS2 9JT, UK*
[*]*Corresponding authors: mbelkin@seas.harvard.edu, capasso@seas.harvard.edu*

Abstract: We report terahertz quantum cascade lasers operating in pulsed mode at an emission frequency of 3 THz and up to a maximum temperature of 178 K. The improvement in the maximum operating temperature is achieved by using a three-quantum-well active region design with resonant-phonon depopulation and by utilizing copper, instead of gold, for the cladding material in the metal-metal waveguides.

OCIS codes: (140.3070) Infrared and far-infrared lasers; (140.5960) Semiconductor lasers; (230.5590) Quantum-well devices.

References and links

1. R. Köhler, A. Tredicucci, F. Beltram, H. E. Beere, E. H. Linfield, A. G. Davies, D. A. Ritchie, R. C. Iotti, and F. Rossi, "Terahertz semiconductor-heterostructure laser," Nature **417,** 156 (2002).
2. B. S. Williams, H. Callebaut, S. Kumar, Q. Hu, and J. L. Reno, "3.4-THz quantum cascade laser based on longitudinal-optical-phonon scattering for depopulation," Appl. Phys. Lett. **82,** 1015 (2003).
3. B. S. Williams, S. Kumar, H. Callebaut, Q. Hu, and J. L. Reno, "Terahertz quantum-cascade laser at $\lambda \approx$ 100 μm using metal waveguide for mode confinement," Appl. Phys. Lett. **83,** 2124–2126 (2003).
4. B. S. Williams, S. Kumar, Q. Hu, and J. L. Reno, "Operation of terahertz quantum-cascade lasers at 164 K in pulsed mode and at 117 K in continuous-wave mode," Opt. Express **13,** 3331 (2005).
5. A. Tredicucci, L. Mahler, T. Losco, J. Xu, C. Mauro, R. Köhler, H. E. Beere, D. A. Ritchie, and E. H. Linfield, "Advances in THz quantum cascade lasers: fulfilling the application potential," Proc. SPIE **5738,** 146 (2005).
6. C. Walther, M. Fischer, G. Scalari, R. Terazzi, N. Hoyler, and J. Faist, "Quantum cascade lasers operating from 1.2 to 1.6 THz," Appl. Phys. Lett. **91,** 131122 (2007).
7. B. S. Williams, "Terahertz Quantum Cascade Lasers," Nature Photon. **1,** 517-525 (2007).
8. K. Unterrainer, R. Colombelli, C. Gmachl, F. Capasso, H. Y. Hwang, D. L. Sivco, and A. Y. Cho, "Quantum cascade lasers with double metal-semiconductor waveguide resonators," Appl. Phys. Lett. **80,** 3060 (2002).
9. S. Kohen, B. S. Williams, and Q. Hu, "Electromagnetic modeling of terahertz quantum cascade laser waveguides and resonators," J. Appl. Phys. **97,** 053106 (2005).
10. S. Kumar, B. S. Williams, Q. Qin, A. W. M. Lee, Q. Hu, J. L. Reno, Z. R. Wasilewski, H. C. Liu, "Terahertz quantum-cascade lasers with resonant-phonon depopulation: high temperature and low-frequency operation," in *Proceedings of the Ninth International Conference on Intersubband Transitions in Quantum Wells*, D. Indjin, Z. Ikonic, P. Harrison, and R.W. Kelsall, eds. (University of Leeds, Leeds, U.K., 2007), p. T16.
11. K. N. Chen, A. Fan, C. S. Tan, R. Reif, and C. Y. Yen, "Microstructure evolution and abnormal grain growth during copper wafer bonding," Appl. Phys. Lett. **81,** 3774 (2002).
12. M. Bahriz, V. Moreau, J. Palomo, R. Colombelli, D. A. Austin, J. W. Cockburn, L. R. Wilson, A. B. Krysa, J. R. Roberts, "Room-temperature operation of $\lambda \approx 7.5$ μm surface-plasmon quantum cascade lasers," Appl. Phys. Lett. **88,** 181103 (2006).
13. M. A. Ordal, R. J. Bell, R. W. Alexander, Jr., L. L. Long, and M. R. Querry, "Optical properties of fourteen metals in the infrared and far infrared: Al, Co, Cu, Au, Fe, Pb, Mo, Ni, Pd, Pt, Ag, Ti, V and W," Appl. Opt. **24,** 4493 (1985).
14. M. Born and E. Wolf, *Principles of Optics* (Cambridge University Press, 1999).
15. "Electrical Resistivity of Pure Metals," in *CRC Handbook of Chemistry and Physics, 88th Edition (Internet Version 2008)*, D. R. Lide, ed. (CRC Press/Taylor and Francis, Boca Raton, Fla., 2008).

#90169 - $15.00 USD Received 26 Nov 2007; revised 11 Jan 2008; accepted 12 Jan 2008; published 25 Feb 2008

16. H. Luo, S. R. Laframboise, Z. R. Wasilewski, G. C. Aers, H. C. Liu, J. C. Cao, "Terahertz quantum-cascade lasers based on a three-well active module," Appl. Phys. Lett. **90,** 041112 (2007).
17. J. Faist, "Wallplug efficiency of quantum cascade lasers: Critical parameters and fundamental limits," Appl. Phys. Lett. **90,** 253512 (2007).

1. Introduction

Terahertz (THz) quantum cascade lasers (QCLs) are an emergent compact source for narrowband THz radiation in the wavelength range ~60–300 μm (~1–5 THz) [1-7]. Currently, these devices operate only at cryogenic temperatures, which limit their usefulness in applications such as spectroscopy, heterodyne detection, and screening. To achieve good performance in these devices, the optical mode must be strongly confined within the active region. This is a challenge because the active region thickness is effectively limited to ~10 μm, owing to the time taken to grow the material by techniques such as molecular beam epitaxy (MBE), and this thickness is an order of magnitude smaller than the free space emission wavelength. As a result, advances in waveguide design have been critical in advancing THz QCL performance. In particular, the implementation of the semi-insulating surface-plasmon waveguide was crucial for the demonstration of the first THz QCL [1]. Improvements in the temperature performance of THz QCLs were further achieved with the development of the metal-metal (MM) waveguide design [3,4,8], which consists of metal films on both sides of the active region and which provides a mode confinement factor of nearly 100% [9]. Currently, a highest operating temperature of 169 K has been achieved in THz QCLs with MM waveguides and an active region based on a resonant-phonon depopulation scheme [4,10]. Copper-to-copper thermocompression wafer bonding [4,11] was used to fabricate these waveguides [4,10] in order to improve their thermal properties, compared to waveguides processed with indium-gold bonding [3,8]. However, the top metal cladding in these devices was made of gold to allow dry-etching of ridges, using the top contact as a self-aligned mask [3,4].

Further improvements in the maximum operating temperatures of THz QCLs can be achieved by improving both the active region and waveguide designs. In THz QCLs with MM waveguides, 30-70% of the waveguide losses may originate from the losses associated with the metal claddings, the precise value depending on the emission wavelength, the active region design, and doping (see Ref. [3] and Fig. 1). The optical losses of the metal cladding can vary depending on the type of metal used [12]. In Fig. 1, we compare the

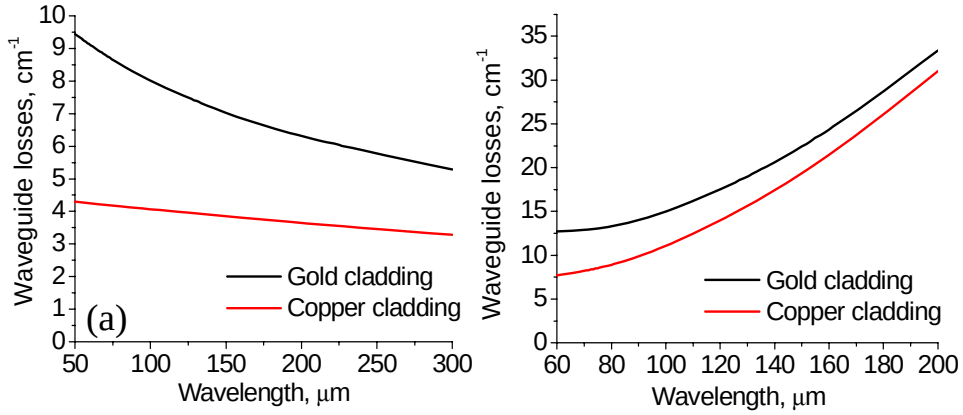

Fig. 1. (a). Calculated waveguide losses for different wavelengths in a metal-metal waveguide assuming a "lossless" active region. (b) Calculated waveguide losses in a metal-metal waveguide assuming a realistic active region design with an average doping of $5x10^{15}$ cm^{-3}. We note that long-wavelength, λ>200 μm, QCLs typically use lower doped active regions.

#90169 - $15.00 USD Received 26 Nov 2007; revised 11 Jan 2008; accepted 12 Jan 2008; published 25 Feb 2008

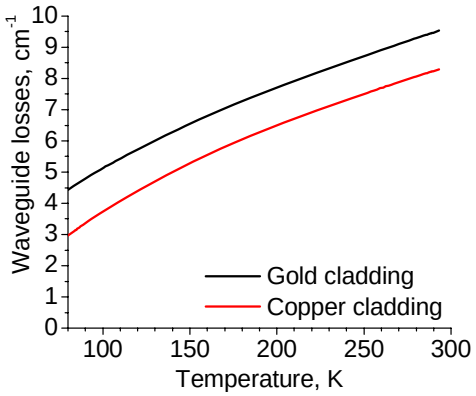

Fig. 2. Calculated temperature dependence of waveguide losses for 100 μm wavelength in a metal-metal waveguide assuming a "lossless" active region. Optical constants of metals were estimated using Eq. (1). The data for temperatures below 80 K is very sensitive to the purity of metals and is not shown.

calculated waveguide losses for 10μm-thick and infinitely wide MM THz QCL waveguides with claddings made of gold and copper. For the data shown in Fig. 1(a), we considered a "lossless" active region with a refractive index of 3.5; for the data shown in Fig. 1(b), we considered an active region doped to 5×10^{15} cm^{-3}, which is a typical average doping level for QCLs emitting between 2 – 5 THz, see, e.g., Ref. [4]. In both cases, a one-dimensional waveguide solver was used for the calculations and the optical constants for the metals were taken from Ref. [13], with the refractive index of the QCL active region being calculated using the Drude-Lorentz approximation with parameters taken from Ref. [9]. The thin contact layers of highly-doped GaAs and the thin metal layers of titanium or tantalum present in real devices were ignored as they were calculated to give negligible contributions to the waveguide losses.

The optical constants of metals, reported in Ref. [13], were measured at room temperature. Because the properties of metals change with temperature, it may be possible that MM waveguides with gold claddings have comparable or lower waveguide losses than MM waveguide with copper claddings at THz QCL operating temperatures. To estimate the temperature dependence of the optical constants of copper and gold, we used an approximate expression [14]:

$$\mathrm{Re}(n) \approx \mathrm{Im}(n) \approx \sqrt{\frac{2\pi\sigma}{\omega}} \qquad (1)$$

where Re(n) and Im(n) are the real and imaginary part of the refractive index of a metal, σ is the electrical conductivity of the metal, and ω is the frequency of light. The electrical conductivities of copper and gold, measured at different temperatures, are well-known [15]. In Fig. 2, we plot the temperature dependence of the optical losses at 3 THz for 10μm-thick and infinitely wide MM waveguides with claddings made of gold and copper, calculated using the optical constants of metals obtained with Eq. (1). The data indicate that MM waveguides with copper claddings have smaller optical losses than MM waveguides with gold claddings even at cryogenic temperatures.

The data in Figs. 1 and 2 demonstrate that, by using copper instead of gold, the waveguide losses in MM THz QCL waveguides can be significantly reduced. We also calculated the optical losses for MM THz waveguides with a silver cladding, using data from Ref. [13], and obtained that the waveguide losses are larger than those in copper MM waveguides. Silver also has smaller electrical conductivity than copper at temperatures up to ~180 K. We note, however, that the optical properties of metals in the THz frequency range have not been extensively studied, and vary with temperature, layer deposition quality, metal purity, and other empirical parameters.

#90169 - $15.00 USD Received 26 Nov 2007; revised 11 Jan 2008; accepted 12 Jan 2008; published 25 Feb 2008

2. Device structure, fabrication, and experimental results

To demonstrate the effect of the waveguide cladding material on the temperature performance of MM THz QCLs, we compared the performance of two sets of devices processed from the same active region material, but with two different MM waveguide cladding metals: gold and copper. The active region in our lasers was based on the three-well resonant-phonon design reported in Ref. [16]. This design may have several advantages compared to the four-well resonant-phonon active region design reported in [4]; the conduction band diagrams for both designs are shown in Fig. 3. In comparison to the four-well design, the three-well design has a simplified injector that may reduce the laser mode absorption losses in the injector states [16], improve the gain linewidth, and allow for higher current throughput [17], whilst still providing comparable injection efficiency into the upper laser level under the operating bias voltage. We note that both designs have similar (to within 1 Å) injection and extraction barrier thicknesses, emission frequencies, and dipole matrix elements for the laser transition.

The QCL material was grown by MBE on an undoped GaAs substrate; the growth sequence started with a 250nm-thick undoped GaAs buffer layer, and was followed by a 300nm-thick $Al_{0.5}Ga_{0.5}As$ etch-stop layer, a 75nm-thick layer of GaAs n-doped to $5x10^{18}$ cm^{-3}, 226 stages of an active region design identical to that of Ref. [16] but with a doping sheet density of $n_s=2.75x10^{10}$ cm^{-2}, and finally a 50nm-thick GaAs layer n-doped to $5x10^{18}$ cm^{-3}. The material was processed into MM waveguides following the procedure outlined in Refs. [3,8]. First, half of a square centimeter of QCL material was cleaved and either Ti/Au (20 nm / 1000 nm) or Ta/Cu (20 nm / 1000 nm) deposited by electron-beam evaporation. The wafers were then manually bonded on a hot plate at 250°C to a highly doped GaAs substrate with deposited layers of Ti/Au/In (20 nm / 75 nm / 1400 nm). The bonded QCL wafer was next lapped down and wet-etched to the etch-stop layer with a hydrogen peroxide/ammonium hydroxide solution (19:1 in volume), and the etch stop layer was stripped with concentrated hydrofluoric acid. The laser ridges, with widths ranging from 25 to 150 μm, were defined using dry etching with a SU-8 2005 photoresist mask. After SU-8 removal, metal (Ti/Au, 10/120 nm or Ta/Cu/Au, 15/90/30 nm) was evaporated on top of the laser ridges. A gold capping was added to the waveguides with copper cladding to avoid copper oxidation and facilitate wire bonding. The processed wafers were finally cleaved into approximately 1.5mm-long bars and indium-mounted onto gold-plated copper blocks. Both the gold and copper processing resulted in robust devices that were easy to wire-bond.

Devices were tested in pulsed mode with 30 ns pulses at a 1 kHz repetition rate. Peak powers were measured with a calibrated helium-cooled bolometer using two 2" diameter

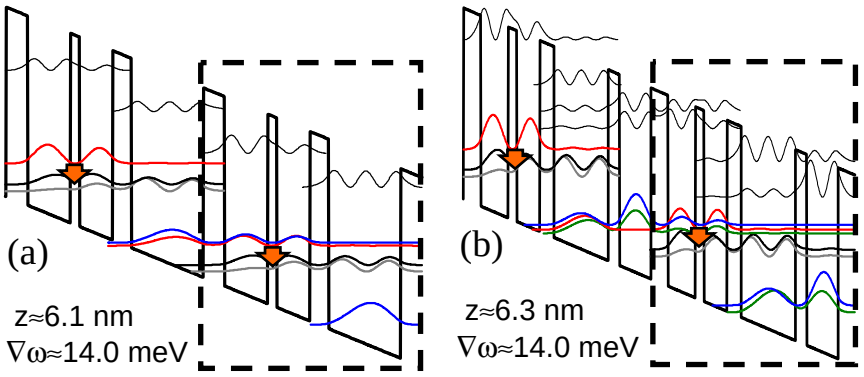

Fig. 3. Conduction band diagrams of (a) three- and (b) four-quantum-well resonant-phonon active region designs, reported in Refs. [16] and [4] respectively. A single quantum-cascade stage is marked by a box. Both structures utilized the $GaAs/Al_{0.15}Ga_{0.85}As$ material system. The layer sequences, starting from the injection barrier, are 48/96/20/74/42/161 Å for (a) and 49/79/25/66/41/156/33/90 Å for (b). Laser transitions are shown with arrows. Also shown are the transition dipole moments and emission energies for the laser transitions, calculated for single isolated modules of the structures. The four-quantum-well resonant-phonon active region design is shown for reference only; it is not used in our experiments.

#90169 - $15.00 USD Received 26 Nov 2007; revised 11 Jan 2008; accepted 12 Jan 2008; published 25 Feb 2008

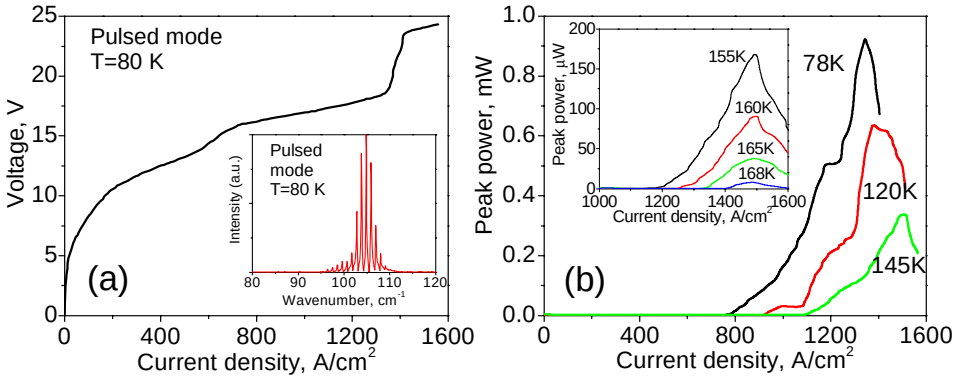

Fig. 4. (a). Current density-voltage characteristic and an emission spectrum (inset) of a representative device processed with a gold metal-metal waveguide. Devices processed with a copper metal-metal waveguides displayed similar current density-voltage characteristics and emission spectra. (b) Light intensity-current density (LI) characteristics of the best-performing device with a gold metal-metal waveguide, 1.3mm-long and 150μm-wide. Inset: the LI characteristics of the device close to the maximum operating temperature of 168 K. The data are not corrected for an estimated 10% power collection efficiency.

parabolic mirrors: one with a 5 cm focal length to collect light from the device and the other with a 15 cm focal length to refocus it onto the detector. Figure 4(a) displays the current density-voltage (I-V) characteristic of a representative device with gold cladding layers, as well as a typical emission spectrum. A step associated with the injector state aligning with the upper laser state can be clearly seen in the I-V characteristics at a current density of approximately 700 A/cm^2; a second step in the I-V characteristics, at a current density of approximately 1350 A/cm^2, is due to the misalignment of the injector and the upper laser states. Devices processed into MM waveguides with a gold cladding typically operated up to 160-164 K. The light output as a function of current density (L-I) for the best performing device with gold MM waveguides, which operated up to 168 K, is shown in Fig. 4(b). We note that the gold MM waveguide devices reported in the original publication [16] operated

#90169 - $15.00 USD Received 26 Nov 2007; revised 11 Jan 2008; accepted 12 Jan 2008; published 25 Feb 2008

only up to 142 K. The improved performance of our devices may stem from a better growth

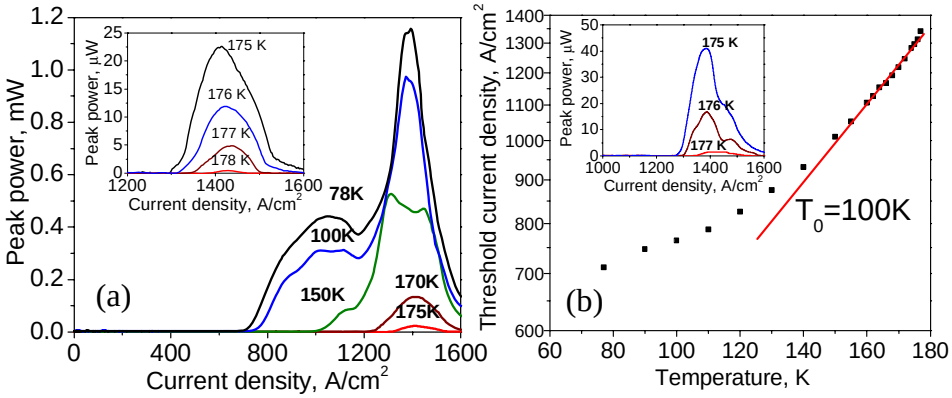

Fig. 5. (a). The LI characteristics of a 1.4mm-long and 125μm-wide device with a copper metal-metal waveguide. Inset: the LI characteristics of the device close to the maximum operating temperature of 178 K. The data are not corrected for an estimated 10% power collection efficiency. Dips in the LI characteristics at current density ~1150 A/cm^2 are due to some of the laser emission lines coincide with atmospheric absorption lines. (b) Threshold current density as a function of temperature for the device in (a). Inset: the LI characteristics of another device with a copper metal-metal waveguide, 1.6mm-long and 100μm-wide, close to its maximum operating temperature of 177 K.

and/or processing quality, as well as lower doping density. Devices processed into MM waveguides with copper cladding typically operated up to 170-174 K. The L-I characteristics for the best-performing device with copper cladding, which operated up to 178 K, are shown in Fig. 5(a), with the dependence of threshold current density on temperature being shown in Fig. 5(b). At high temperatures, the threshold current density displays an asymptotic dependence of *~exp(T/T$_0$)* with T$_0$≈100 K. We observed a similar asymptotic dependence with similar T$_0$ for devices processed into MM waveguides with gold cladding.

3. Discussion

We attribute the observed improvement in temperature performance in copper MM waveguide devices to the superior optical properties of copper over those of gold. The differences in thermal properties between gold and copper are not expected to play an important role in determining the device performance since both copper and gold MM waveguide devices were processed following the same indium-bonding procedure and tested in pulsed mode with very short current pulses. We note that good thermal packaging is necessary for good continuous-wave (CW) performance, such as that reported in Ref. [4] where copper-to-copper thermocompression wafer bonding was utilized. Our results indicate that, for the best CW performance, one may want to modify the processing procedure reported in Ref. [4] to include a layer of copper in the top waveguide cladding for low-loss plasmon wave guiding.

The exact degree of improvement in temperature performance of a QCL owing to the reduction of waveguide losses depends on the characteristic temperature T$_0$ of the active region. To a first approximation, we can assume that the waveguide losses do not change with temperature and, at high temperatures, the maximum laser gain scales with temperature as *~exp(-T/T$_0$)*, where T$_0$ is the characteristic temperature deduced from the dependence of the threshold current density on temperature. Under these assumptions and neglecting small mirror losses in the MM waveguides [9], the maximum operating temperatures for the devices with copper and gold waveguide claddings should scale as:

$$T_{\max}(Cu) - T_{\max}(Au) = T_0 \times \ln\left(\frac{\alpha(Au)}{\alpha(Cu)}\right) \quad (1)$$

#90169 - $15.00 USD Received 26 Nov 2007; revised 11 Jan 2008; accepted 12 Jan 2008; published 25 Feb 2008

where $T_{max}(Au)$, $T_{max}(Cu)$, $\alpha(Au)$, and $\alpha(Cu)$ are the maximum operating temperatures and waveguide losses for the MM waveguides with claddings made of gold and copper, respectively. Thus, for a given reduction in the waveguide losses, one may expect a larger improvement in the maximum operating temperatures for devices with larger T_0.

In the case of our devices, Eq. (1) suggests that the substitution of gold with copper for the waveguide cladding resulted in an approximately 10% reduction in the waveguide losses. Similar results can be obtained by comparing the threshold current densities for the devices reported in Figs. 4(b) and 5(a). A 10% reduction in the waveguide losses is smaller than that expected from the data in Fig. 1 (~30%); the discrepancy is likely to stem from uncertainties in the real values of the optical constants of the metals and the QCL active region, as well as from losses introduced by imperfect processing.

4. Conclusion

We have demonstrated that substitution of gold for copper in MM THz QCL waveguides results in a reduction of the waveguide losses, which helps to increase the maximum operating temperatures of these devices. The processing procedures for the MM waveguides with copper and gold claddings are similar, and the devices with copper MM waveguides are robust and easy to wire-bond. Our MM THz QCLs with copper cladding, and an active region based on the three-quantum-well resonant-phonon depopulation design [16], operated in pulsed mode up to the highest recorded temperature for THz QCLs to date, 178 K.

Acknowledgments

The structures were processed in the Center for Nanoscale Science (CNS) in Harvard University. Harvard-CNS is a member of the National Nanotechnology Infrastructure Network. Harvard University acknowledges support from the AFOSR under Contract No. FA9550-05-1-0435 (Gernot Pomrenke). J. F. acknowledges support from the NSF Graduate Fellowship. The University of Leeds acknowledges support from EPSRC (U.K.) and Her Majesty's Government Communications Centre.

#90169 - $15.00 USD Received 26 Nov 2007; revised 11 Jan 2008; accepted 12 Jan 2008; published 25 Feb 2008